Adhesive and Cohesive Cracking Analysis of Asphalt Mastics in Contact with Steel Substrates Using an Energy-Based Crack Initiation Criterion

Supplementary material

S1. Uniaxial tensile tests of mastics under various factors

Table S1 Uniaxial tensile tests of mastics under various factors

Factors	Test configurations				
	Materials	Filler concentration (%)	Thickness (μm)	Strain rate (s^{-1})	Temperature (℃)
Sample thickness	Bitumen	0	50–200	0.02	30
Strain rate	Mastic	33	160	0.01–0.31	30
Temperatures	Mastic	33	200	0.1	20–35
Filler concentration	Mastic	0–60	300	0.05	35

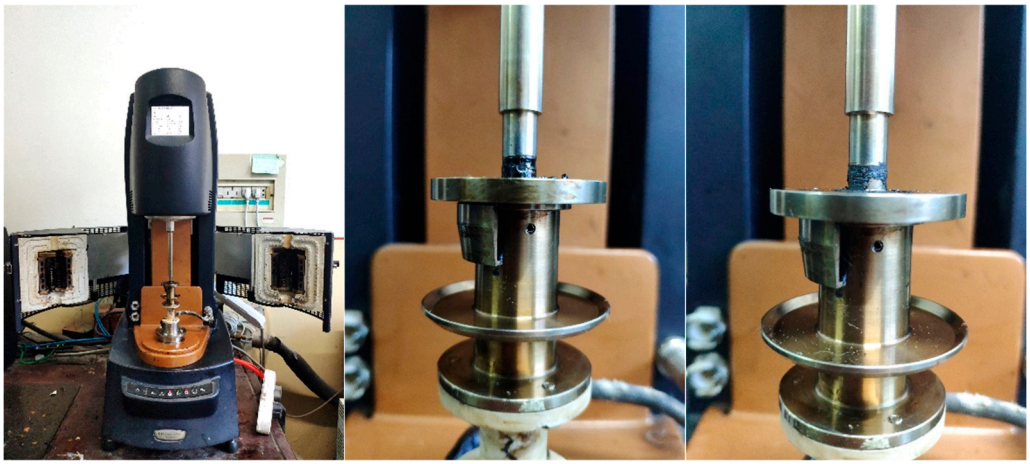


Figure S1. The uniaxial tensile test and different mastic samples

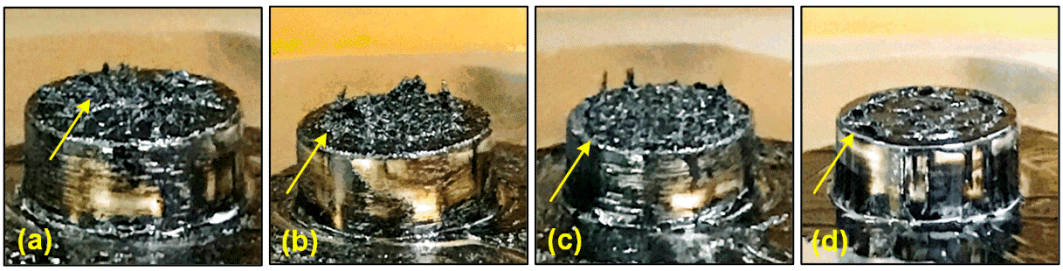


Figure S2. A group of the failed mastic samples with adhesive and cohesive cracking

S2. The surface free energy components of probe liquids for surface free energy measurements

Table S2 Surface free energy components of probe liquids at 25 °C

Probe liquids	γ_L (mJ/m^2)	γ_L^{LW} (mJ/m^2)	γ_L^{AB} (mJ/m^2)	γ_L^+ (mJ/m^2)	γ_L^- (mJ/m^2)
Distilled water	72.80	21.80	51.00	25.50	25.50
Glycerol	64.00	34.00	30.00	3.92	57.40
Ethylene glycol	48.00	29.00	19.00	1.92	47.00
20 wt% ethanol solution	42.00	19.00	23.00	11.50	11.50

S3. Demonstration of relaxation modulus calculation

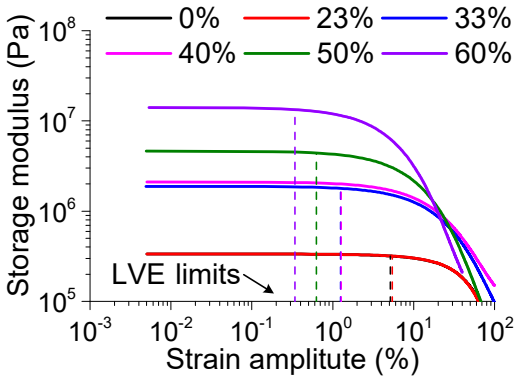


Figure S3. Relationship between complex modulus and strain amplitude at 25°C and 10 rad/s and linear viscoelastic (LVE) limits

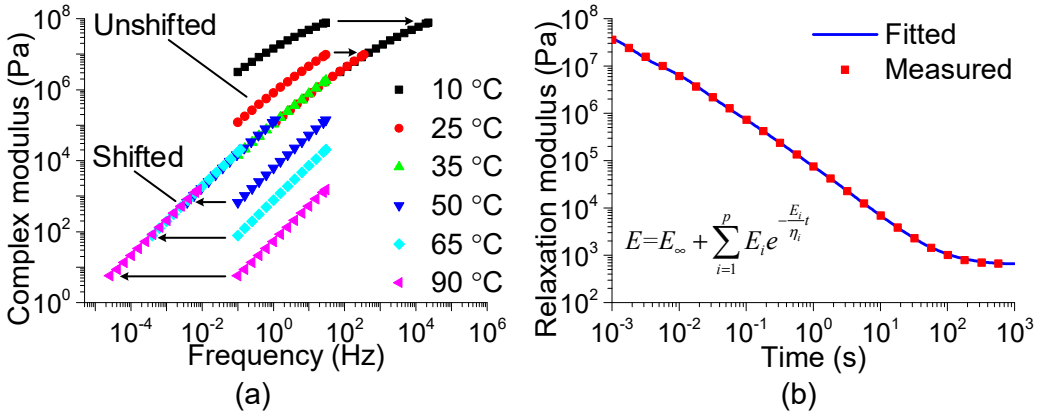


Figure S4. Relaxation modulus determination at 35 °C using frequent sweep tests. (a) is a typical master curve and (b) is the relaxation modulus fitted by generalized Maxwell model.

Table S3 Generalized Maxwell model parameters of mastics with various filler concentrations at 35°C

Spring parameters						
Mastics V_{Filler} (%)*	0	23	33	40	50	60
E_∞ (Pa)	0.8	0.6	1.5	5.0	35732.0	1800.0
E_1 (Pa)	18.5	91.0	72.7	547.0	2397.6	8789.1
E_2 (Pa)	3.4	3.8	3.8	4.0	19018.3	23425.5
E_3 (Pa)	120.0	606.0	565.0	2730.0	559.0	49313.3
E_4 (Pa)	66.3	139.0	128.0	189.0	34664.2	43076.0
E_5 (Pa)	967.0	3320.0	3580.0	13800.0	364.0	132410.5
E_6 (Pa)	423.0	470.0	508.0	551.0	80169.2	526.6
E_7 (Pa)	6510.0	15600.0	20200.0	57800.0	395.5	376278.7
E_8 (Pa)	28000.0	60300.0	92000.0	222000.0	390586.5	246.0
E_9 (Pa)	2230.0	2480.0	2560.0	2670.0	390586.5	715891.0
Dashpot parameters						
Mastics V_{Filler} (%)*	0	23	33	40	50	60
η_1 (Pa·s)	584.0	2880.0	2300.0	17300.0	2397599.3	1562949.5
η_2 (Pa·s)	61.3	66.7	68.0	70.3	6014122.4	2342549.4
η_2 (Pa·s)	1200.0	6060.0	5650.0	27300.0	99397.2	1559422.8
η_3 (Pa·s)	373.0	784.0	720.0	1060.0	1949308.7	766011.8
η_4 (Pa·s)	3060.0	10500.0	11300.0	43700.0	2046.9	1324104.9
η_5 (Pa·s)	752.0	836.0	903.0	980.0	253517.1	2961.3
η_6 (Pa·s)	6510.0	15600.0	20200.0	57800.0	703.4	1189897.6
η_7 (Pa·s)	8870.0	19100.0	29100.0	70100.0	123514.3	437.4
η_8 (Pa·s)	397.0	441.0	455.0	474.0	123514.3	715891.0

* V_{Filler} (%)is the filler volumetric concentrations of mastics.

S4. Measured stress and linear viscoelastic stress curves

Considering the inevitable initial stress in tensile tests, the linear viscoelastic stress of mastics is expressed as

$$\sigma_{LV}(t)=\sigma_{initial}+\int_0^t E(t-\tau)\frac{\partial \varepsilon}{\partial \tau}d\tau=\frac{v}{l_0}\left[E_\infty t+\sum_{i=1}^{p}\eta_i\left(1-e^{-\frac{E_i}{\eta_i}t}\right)\right] \tag{S1}$$

where $\sigma_{initial}$ is the initial stress in tensile tests.

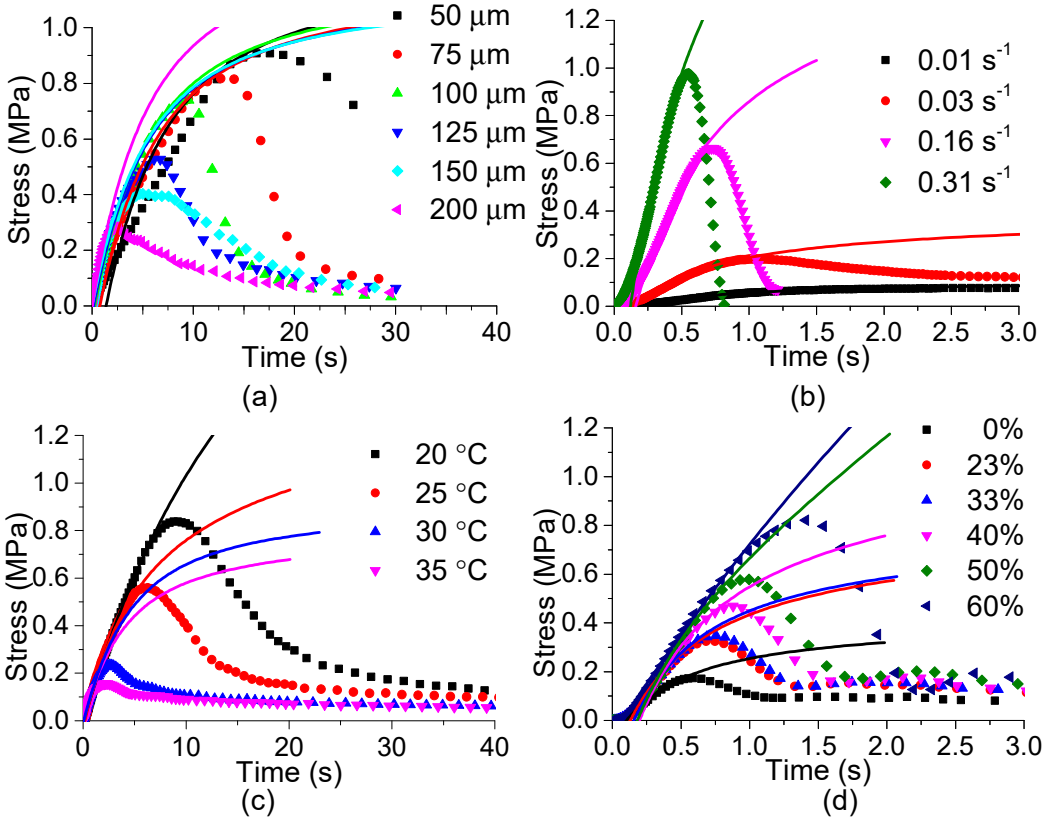


Figure S5. Stress curve against time for (a) the mastics containing 33% filler with various thicknesses at 30 °C and 20 µm/s, (b) the 160 µm mastics with 33% filler concentration at 30 °C and various loading rates, (c) the 200 µm mastics with 33% filler concentration at various temperatures and 20 µm/s and (d) the 300 µm mastics with various filler concentrations at 35 °C and 15 µm/s.

S5. Correlation of crack stress and tensile strength with average initial crack size

To normalize the crack stress, tensile strength and average initial crack size of different mastics under diverse conditions, an index is defined as the ratio of variables and a reference value. Specifying the first value as the reference variable under various factors, the cracking stress ratios, tensile strength ratios, and average initial crack size ratios were calculated and plotted at double logarithm coordinates in Fig. S4. The cracking stress ratios and tensile strength ratios were fitted by power functions of the average initial crack size ratio. The fitted curves reach a good agreement with the measured data. A negative exponent indicates that a larger initial crack size results in lower cracking stress and tensile strength. Additionally, the power functions indicate the steeper slopes of cracking stress and tensile strength for smaller

average initial crack size but plateaus for a large initial crack size.

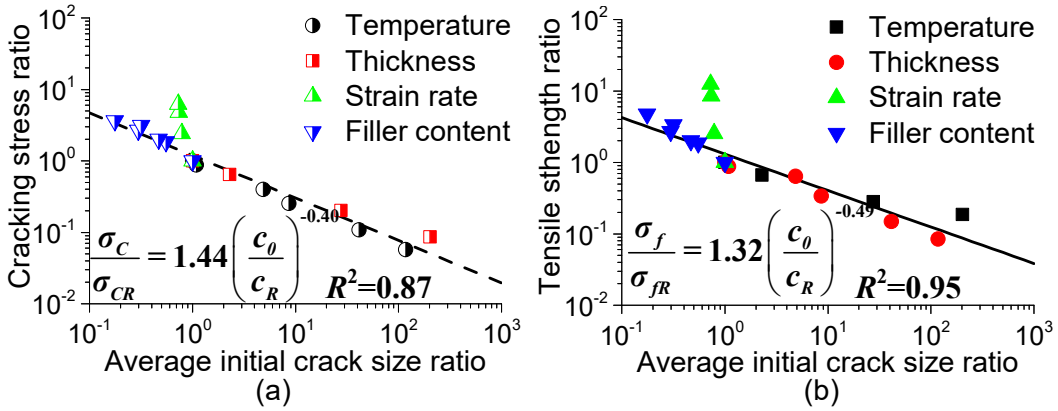


Figure S6. The cracking stress ratio and tensile strength ratio versus the average initial crack size ratio at double logarithm coordinates.